

## Calculation of the electric field in interference coatings

© E.N. Kotlikov<sup>1</sup>, A.N. Tropin<sup>2,¶</sup>

<sup>1</sup> Saint-Petersburg State University of Aerospace Instrumentation, St. Petersburg, Russia

<sup>2</sup> Joint Stock Company „Girikond „Research Institute“,  
194223 St. Petersburg, Russia

¶ e-mail: 216@giricond.ru

Received April 29, 2022

Revised August 24, 2022

Accepted August 25, 2022

A technique for calculating the electric field in interference coatings is described. The technique is used to find areas in the coating structure with electric field minima. Thin absorbing metal films are introduced into these areas during design. The results of calculating the transmission spectra of narrow-band interference filters with absorbing metal films are presented. It is shown that such metal-dielectric thin-film structures block radiation in the long-wavelength region of the spectrum.

**Keywords:** electromagnetic field amplitude, narrow-band interference filters, spectra, films, absorption, transmission.

DOI: 10.21883/EOS.2022.11.55112.3630-22

### Introduction

Transmission and reflection spectra of a thin-film metal-dielectric coating containing nonabsorbing dielectric materials and absorbing metal films are considerably different from spectra of the same interference coating but without absorbing films. This can be used to produce structures with required spectral characteristics. In [1,2] synthesis of narrow-band interference filters (IF) is described, where thin absorbing metal films are used. This type of structures allows blocking the radiation in a spectral range of wavelengths greater than the wavelength of transmission maximum of the interference filter. In the synthesis of antireflection coatings, the introduction of thin absorbing films allows reducing the reflection and expanding the range of suppression of the reflected radiation [3].

In the optics of thin films the problem of analysis of the electric field strength distribution in the coating structure has been arisen before as well. In particular, in [4] the analysis of electric field strength is used to improve radiation resistance of interference coatings. In [5] absorbing films were used to reduce reflection in interference filters. In [6] absorbing films were used in interferometers of reflected light.

The optimization procedures traditionally used to search for solutions not always yield satisfactory results in the case of metal-dielectric coatings. Therefore, an additional analysis is required that consists in calculation of the electric field strength distribution within the multilayered structure.

In this study a technique is described to calculate electric field in interference structures using the formalism proposed by Abeles [7]. The technique is used to find out the regions in structures of multilayered thin-film coatings, where minima of electric field strength are observed. These regions were designed with thin absorbing metal

films and transmission and reflection spectra of interference coatings were calculated.

### The electric field strength calculation technique

The electric field strength was calculated using the following model of multilayered thin-film coating [7–9]:

- normal incidence of radiation, its direction is shown by arrow in Fig. 1;
- no absorption in dielectric films and in the substrate;
- each layer with number  $j$  is characterized by a refractive index of  $n_j$  and a physical (geometric) thickness of  $d_j$ ;
- the substrate is characterized by the refractive index  $n_s$ ;
- layers are numbered starting from the substrate towards the air, i.e. the layer adjacent to the substrate has number 1. The layer in contact with the air has the highest number;
- for the graphical representation of field distribution inside the multilayered coating the count starts from the

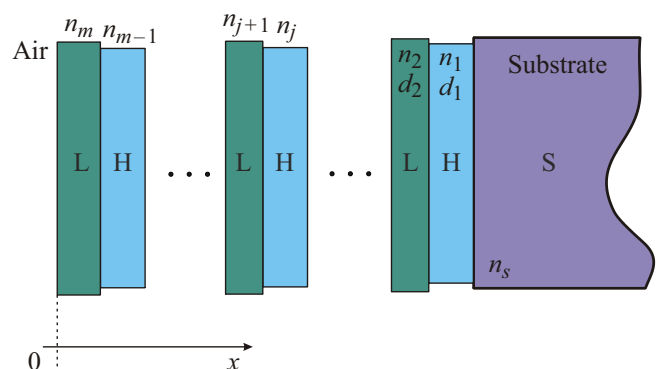


Figure 1. Model of multilayered thin-film coating.

„air–last layer“ interface. That is, the field with current coordinate  $x$  corresponds to the field in the space point at a distance of  $x$  from the „air–last layer“ interface (Fig. 1).

Characteristic matrix  $M_j$  of the layer with number  $j$  can be written as follows (see, for example, [9]):

$$M_j = \begin{bmatrix} \cos \beta_j & \frac{i}{n_j} \sin \beta_j \\ in_j \sin \beta_j & \cos \beta_j \end{bmatrix}, \quad (1)$$

where  $i$  is imaginary unit, and phase (phase thickness)  $\beta_j$  is equal to:

$$\beta_j = \frac{2\pi}{\lambda} n_j d_j, \quad (2)$$

where  $n_j$  is refractive index of the layer with number  $j$  at a wavelength of  $\lambda$ ,  $d_j$  is geometric thickness of the layer with number  $j$ .

If the layer thickness  $d_j$  is not defined in units of physical thickness in the calculation, but in  $\lambda_0/4$  quarter-wavelengths as an optical thickness, then phase  $\beta_j$  can be written as follows:

$$\beta_j = \frac{2\pi}{\lambda} n_j \frac{\lambda_0}{4n_0} D_j, \quad (3)$$

where  $\lambda_0$  is reference (basic) wavelength,  $n_{0j}$  is refractive index of the layer with number  $j$  at a wavelength of  $\lambda_0$ ,  $D_j$  is optical thickness of the layer with number  $j$  in fractions of  $\lambda_0/4$ .

The characteristic matrix of a multilayered structure  $G$  that contains  $m$  layers can be written as a product of multiplication of characteristic matrices of individual layers. In this case multiplication of matrix of the layer with increasing number takes place from the left [9]:

$$G = M_m M_{m-1} \cdots M_j M_{j-1} \cdots M_2 M_1 = \prod_{j=m}^1 M_j \begin{bmatrix} g_{11} & ig_{12} \\ ig_{21} & g_{22} \end{bmatrix}, \quad (4)$$

where  $i$  is imaginary unit.

Components of the  $G$  matrix allows calculating amplitude and phase spectra of Fresnel reflection and transmission coefficients of a multilayered thin-film coating shown in Fig. 1.

Along with building up the distribution of actual electric field amplitude in a point with  $x$  coordinate, in the case under consideration it is convenient to use the squared electric field amplitude in a point with coordinate  $x$  normalized to the squared incident wave field amplitude [4,7,8]:

$$N(x) = \frac{|E(x)|^2}{|E_0^+|^2}, \quad (5)$$

where  $E(x)$  is electric field amplitude in a point with current coordinate  $x$ ,  $E_0^+$  is field amplitude of the wave incident from the external environment (the air) onto the optic coating.

The denominator in (5), expressed in terms of components of the  $G$  matrix, has the following form [4,7]:

$$|E_0^+|^2 = \frac{1}{4} \left( \left( g_{11} + g_{22} \frac{n_s}{n_0} \right)^2 + \left( \frac{1}{n_0} g_{21} + g_{12} n_s \right)^2 \right) \frac{|E|^2}{2}, \quad (6)$$

where  $n_s$  is refractive index of the substrate at a wavelength of  $\lambda$ ,  $n_0$  is refractive index of the external environment ( $n_0 = 1$  for the model represented in Fig. 1),  $E$  is electric field strength of the passed wave.

Now we derive a formula for the numerator in (5), i.e. we calculate the electric field strength at a distance of  $x$  from the „air–last layer“ interface.

For this purpose, let us multiply from the left the special matrix  $G_{inv}$  [7] by the characteristic matrix of the multilayered coating  $G$ :

$$G_{inv} G = \begin{bmatrix} g'_{11} & ig'_{12} \\ ig'_{21} & g'_{22} \end{bmatrix} \begin{bmatrix} g_{11} & ig_{12} \\ ig_{21} & g_{22} \end{bmatrix} = \begin{bmatrix} g''_{11} & ig''_{12} \\ ig''_{21} & g''_{22} \end{bmatrix}, \quad (7)$$

where matrix  $G_{inv}$

$$G_{inv} = \begin{bmatrix} \cos \Delta\beta & -\frac{i}{n_j \sin \Delta\beta} \\ -in_j \sin \Delta\beta & \cos \Delta\beta \end{bmatrix} = \begin{bmatrix} g'_{11} & ig'_{12} \\ ig'_{21} & g'_{22} \end{bmatrix}. \quad (8)$$

The matrix  $G_{inv}$  takes into consideration the dependence on coordinate  $x$  as follows:

$$\Delta\beta = \frac{2\pi}{\lambda} n_j x, \quad (9)$$

where  $n_j$  is refractive index in a point of the multilayered coating at a distance of  $x$  from the „air–last layer“ interface.

The required numerator in (5) can be written as:

$$|E(x)|^2 = ((g''_{11})^2 + (n_s g''_{12})^2) \frac{|E|^2}{2}. \quad (10)$$

Then, by substituting (6) and (10) into (5), we get:

$$N(x) = \frac{|E(x)|^2}{|E_0^+|^2} = \frac{(g''_{11})^2 + (n_s g''_{12})^2}{\frac{1}{4} \left( \left( g_{11} + g_{22} \frac{n_s}{n_0} \right)^2 + \left( \frac{1}{n_0} g_{21} + g_{12} n_s \right)^2 \right)}. \quad (11)$$

Expression (11) describes the distribution of squared electric field amplitude in the structure of interference coating.

Using the above-presented equations, a program to calculate  $N(x)C$  was written in Mathcad software package [10]. With this program, the electric field strength was analyzed in structures of two types of narrow-band interference filters, which are different in refractive indices of their central (resonant) layers that define the wavelength of filter's transmission maximum [9,11]. The calculation was used to search for regions in the coating structure with minimum amplitudes of electric field strength. Absorbing metal films were placed in these points to allow forming the required spectral characteristics of the IF.

**Table 1.** Structure of 15-layer IF with low-refractive index half-wave films

|               |     |     |     |     |      |      |     |     |
|---------------|-----|-----|-----|-----|------|------|-----|-----|
| Layer number  | 1   | 2   | 3   | 4   | 5    | 6    | 7   | 8   |
| Material      | Ge  | SiO | Ge  | Ni  | SiO  | Ni   | Ge  | SiO |
| Thickness, nm | 274 | 611 | 276 | 4.9 | 1203 | 22.6 | 219 | 611 |
| Layer number  | 9   | 10  | 11  | 12  | 13   | 14   | 15  | –   |
| Material      | Ge  | SiO | Ge  | Ni  | SiO  | Ni   | Ge  | –   |
| Thickness, nm | 274 | 611 | 274 | 4.9 | 1191 | 14.4 | 274 | –   |

**Synthesis of interference filters**

The procedure of designing an optical interference coating, as a rule, consists of a number of stages. At the initial stage, the requirements for spectral parameters and characteristics of the coating are formulated, film-forming materials available for implementation of the coating are determined, initial structure of the coating is selected to perform further optimization procedure. At the following stage the structure is optimized using various modern tools of multivariable search.

Let us consider synthesis of two interference filters of different types at a wavelength of  $4.27 \mu\text{m}$  ( $2342 \text{ cm}^{-1}$ ), that corresponds to the absorption line of  $\text{CO}_2$ -gas [12]. A combined interference filter was selected as the initial structure, which was composed of two interference filter elements based on Fabry-Pérot interferometer separated by a matching layer [11]. The first type of interference filter used central half-wave layers of films with low refractive index, while the second type used films with high refractive index.

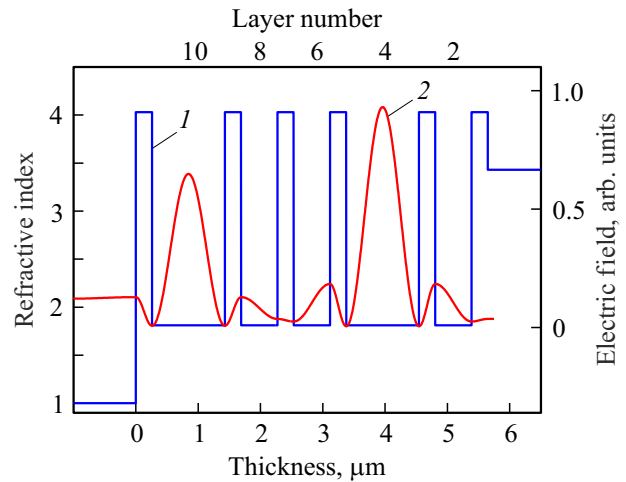
The structure of two-section narrow-band filter without absorbing films for a wavelength of  $4.27 \mu\text{m}$  (wave number  $2342 \text{ cm}^{-1}$ ) had the following form [12]:

$$S-(\text{HL})\text{H}(\mathbf{2L})(\text{HL})^2\text{H}(\mathbf{2L})\text{H}-\text{air}, \quad (13)$$

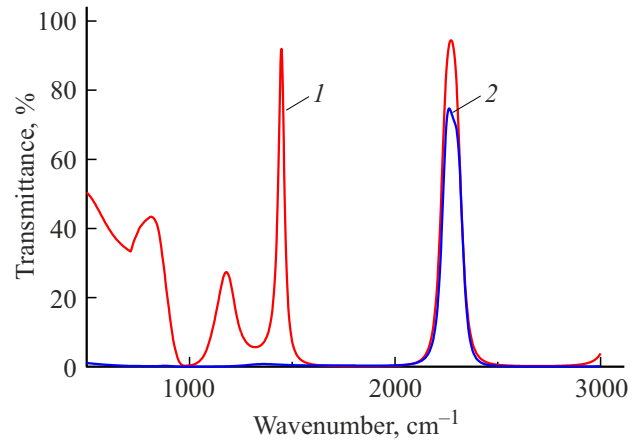
where S is the substrate, H is a quarter-wave layer with high refractive index, L is a quarter-wave layer with low refractive index, air is the ambient air. Optical thicknesses of film L and H corresponds to the quarter-wave layer at a wavelength of  $4.27 \mu\text{m}$ . In the calculations of this study the refractive index of low-refractive layers was assumed equal to 1.81 ( $\lambda = 4.27 \mu\text{m}$ ), that corresponds to Silicon monoxide (SiO) films. The refractive index of high-refractive layers was assumed equal to 4.03 ( $\lambda = 4.27 \mu\text{m}$ ), that corresponds to Germanium (Ge) films. The refractive index of Silicon substrate is 3.43 ( $\lambda = 4-5 \mu\text{m}$ ) [13].

Fig. 2 shows the topology (refractive index as a function of geometric thickness) of multilayer structure (13). Also, Fig. 2 presents the distribution of field  $N(x)$  inside the interference filter.

Fig. 3 (curve 1) shows the transmission spectrum of IF with a maximum corresponding to wave number



**Figure 2.** IF topology (1) and field distribution (2) in a structure with half-wave layers of films with low refractive indices.



**Figure 3.** Transmission spectra of IF with half-wave layers of films with low refractive index. 1 — initial structure, 2 — structure with metal layers from Table 1.

**Table 2.** Structure of 15-layer IF with high-refractive-index half-wave films

|               |     |     |     |    |     |     |     |     |
|---------------|-----|-----|-----|----|-----|-----|-----|-----|
| Layer number  | 1   | 2   | 3   | 4  | 5   | 6   | 7   | 8   |
| Material      | Ge  | SiO | Ge  | Ni | Ge  | SiO | Ge  | SiO |
| Thickness, nm | 274 | 632 | 272 | 13 | 244 | 632 | 274 | 632 |
| Layer number  | 9   | 10  | 11  | 12 | 13  | 14  | 15  | –   |
| Material      | Ge  | SiO | Ge  | Ni | Ge  | SiO | Ge  | –   |
| Thickness, nm | 274 | 632 | 253 | 11 | 250 | 631 | 274 | –   |

$\nu = 2342 \text{ cm}^{-1}$ . In the figure the spectral dependence on wave number is used for clarity. It can be seen that in the spectral range with wave numbers less than  $1667 \text{ cm}^{-1}$  (wavelengths higher than  $6 \mu\text{m}$ ) the filter has transmission up to 85%. The purpose of thin absorbing films introduced

into the structure of such IF is to suppress this undesirable transmission in the long-wave region of the spectrum.

The calculation of electric field distribution in the multilayer thin-film coating that forms the IF shows that the field strength is distributed in a non-uniform manner and has extreme points (minima). Taking this into account, as well as to reduce optical losses in the multilayered system at a wavelength of  $\lambda_{\max}$  with simultaneous blocking of radiation in the long-wave region the metal films must be placed in points of local minima, as it is proposed in [1,2]. Therefore, at the next stage of designing thin films of Nickel with a geometric thickness of  $5\mu\text{m}$  were introduced into the IF structure at the interfaces of 3–4 and 4–5 layers, as well as at the interface of 9–10 and 10–11 layers.

The addition of metal absorbing films shifts the transmission maximum of the interference filter. This shift can be easily compensated either by the central (resonance) layer, or by adjacent layers that form dielectric mirrors. Therefore, at the next stage the obtained structure was optimized with respect to the target spectrum. In the range of  $2000\text{--}2500\text{ cm}^{-1}$  the spectrum of structure of (13) was used as the target spectrum. In the rest of spectral range the transmission was set equal to zero.

Coatings were calculated and optimized using the Film-Manager program [14]. The program provides for calculation of spectra of preset structures, as well as synthesis (optimization) of coatings with characteristics that match the required (target) spectrum as closely as possible.

The IF was optimized (synthesized) by minimizing a fitness function of the following form:

$$F = \sum_{i=1}^N |T_{\text{calc}}(\lambda_i) - T_{\text{et}}(\lambda_i)|^2 W(\lambda_i), \quad (14)$$

where  $T_{\text{calc}}(\lambda_i)$  and  $T_{\text{et}}(\lambda_i)$  are calculated and target (required) values of transmittance factor at wavelengths of  $\lambda_i = \lambda_{\min} + (i - 1)\Delta\lambda$ , respectively,  $\lambda_{\min}$  is the short-wave limit of the spectral interval,  $\Delta\lambda = (\lambda_{\max} - \lambda_{\min})/N$  is increment of the wavelengths grid,  $N$  is the number of points where the spectrum is to be calculated, and  $W(\lambda_i)$  is a user-defined weight coefficient in point  $i$ .

After optimization of structure (13) with metal films a structure represented in Table 1 was obtained.

Spectrum of this coating is shown in Fig. 3 (curve 2). Shape of the transmission profile is the same as that of the filter without metal films. In the spectral range with wave numbers less than  $1667\text{ cm}^{-1}$  ( $\lambda > 6\mu\text{m}$ ) the transmission is below 0.5%. The transmission at the point of maximum is somewhat below than that of the coating without metal films. However, it is practically the same as transmission of the filter without metal films but with an additional light filter that blocks the long-wave region [2].

In addition to the described above, authors have synthesized an interference filter with similar spectral characteristics, but with different coating structure. The difference between the IF structure and the previously considered

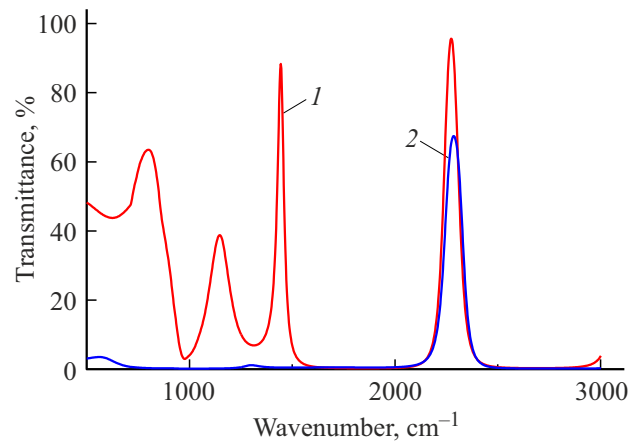


**Figure 4.** Transmission spectra of IF with half-wave layers of films with high refractive index. 1 — initial structure, 2 — structure with metal layers from Table 2.

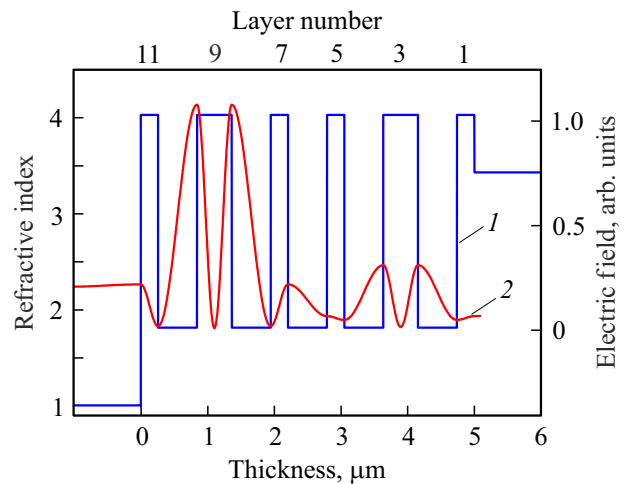


**Figure 5.** IF topology (1) and field distribution (2) in a structure with half-wave layers of films with high refractive indices.

structure was that central half-wave layers were implemented as films with high refractive index.

Initial model structure of the combined narrow-band filter for a wavelength of  $4.27\mu\text{m}$  has the following form:

$$S\text{—}HL(\mathbf{2H})(\text{LH})^2L(\mathbf{2H})\text{LH—air}, \quad (15)$$

where all notations are the same as in (13).

Fig. 4 (curve 1) shows transmission spectrum of this IF. In the spectral region with wave numbers less than  $1667\text{ cm}^{-1}$  (with wavelengths over  $6\mu\text{m}$ ) the IF also has high parasitic (undesirable) transmission.

Fig. 5 shows topology of multilayered structure (15). The same figure presents field distribution  $N(x)$  inside the interference structure.

The calculation of electric field distribution in the multilayer thin-film coating that forms the IF shows that the field strength distribution has extreme points (minima) located in the middle of the separating (half-wave)

films 2H. Taking this into account, thin films of Nickel with a geometric thickness of 5 nm were placed in the middle of half-wave Germanium layers, specifically in the middle of the third and the ninth layers. Then all the structure was optimized to obtain a spectrum that matches the required spectrum as closely as possible.

After optimization of structure (15) with metal films a structure of metal/dielectric IF represented in Table 2 was obtained.

Transmission spectrum of this coating is shown in Fig. 4 (curve). In the long-wave spectral region of radiation suppression the transmission is somewhat higher than that of the structure from Table 1. Reduction of the undesirable transmission becomes possible with the increase in thickness of Nickel metal films, which, however, leads to a significant reduction of transmission at a wavelength of  $\lambda_{\max}$ .

## Conclusion

In this study a technique is considered to calculate electric field in interference coatings, which is based on the mathematical formalism with the use of system response matrices. The technique is used to find out the regions in structures of multilayered thin-film coatings, where minima of electric field strength are observed. Then, at the next stage of designing, thin absorbing metal film are introduced in these regions.

The use of the presented approach allows creating metal/dielectric narrow-band IFs with transmission blocked in the long-wave region of the spectrum without the need for additional blocking filters based on absorbing systems or dielectric mirrors.

The obtained results of IF designing with a transmission maximum at  $\nu = 2342 \text{ cm}^{-1}$  show that for the multilayered coating considered in this study and composed of Germanium films and Silicon monoxide, the addition of several thin layers of Nickel with a thickness from 5 to 25 nm allows practically complete blocking of undesirable transmission in the long-wave region of the spectrum. In this case the localization of metal layers added to the structure coincides with minima of electric field strength of the wave propagating in the interference system.

## Funding

This work was supported by a grant from the Ministry of Science and Higher Education of the Russian Federation.

## Conflict of interest

The authors declare that they have no conflict of interest.

## References

- [1] E.N. Kotlikov. *J. Opt. Techn.*, **88** (6), 321 (2021). DOI: 10.1364/JOT88.000321].
- [2] E.N. Kotlikov, A.N. Tropin. *J. Opt. Techn.*, **88** (9), 543 (2021). DOI: 10.1364/JOT88.000543].
- [3] E.N. Kotlikov. *J. Opt. Techn.*, **87** (11), 693 (2020). DOI: 10.1364/JOT87.000693].
- [4] O. Arnon, P. Baumeister. *Appl. Opt.*, **19** (11), 1853 (1980). DOI: 10.1364/AO.19.001853
- [5] B.T. Sullivan, K.L. Byrt. *Appl. Opt.*, **34** (25), 5684 (1995). DOI: 10.1364/AO.34.005684
- [6] Yu.V. Troitskiy, *Mnogoluchevye interferometry otrazhennogo sveta* (Nauka, Novosibirsk, 1985) (in Russian).
- [7] F. Abeles. *Ann. Phys. (Paris)*, **12** (3), 504 (1948). DOI: 10.1051/anphys/194812030504
- [8] W.N. Hansen. *J. Opt. Soc. Am.*, **58** (3), 380 (1968). DOI: 10.1364/JOSA.58.000380
- [9] M. Born, E. Wolf. *Principles of Optics, 4th rev. ed.* (Pergamon Press, 1970).
- [10] Mathcad [Electronic resource ].  
URL: <https://www.mathcad.com/en/>
- [11] *Spravochnik po lazeram*, v. 1, Ed. A.M. Prokhorov (Sov. Radio, Moskva, 1978) (in Russian).
- [12] N.A. Borisevich, V.G. Vereshchagin, M.A. Validov *Infra-krasnye filtry* (Nauka i tehnika, Minsk, 1971) (in Russian).
- [13] E.N. Kotlikov, Y.A. Novikova. *Opt. Spectrosc.*, **120** (5), 815 (2016). DOI: 10.1134/S0030400X16050167].
- [14] E.N. Kotlikov, I.I. Kovalenko, Yu.A. Novikova, *Inf.-upr. syst.*, **3** (76), 51 (2015), (in Russian), DOI: 10.15217/issn1684-8853.2015.3.51